A single-molecule method for the quantitation of microRNA gene expression

Lori A Neely[1], Sonal Patel[1], Joanne Garver[1], Michael Gallo[2], Maria Hackett[3], Stephen McLaughlin[1], Mark Nadel[1], John Harris[1], Steve Gullans[4] & Jenny Rooke[1]

MicroRNAs (miRNA) are short endogenous noncoding RNA molecules that regulate fundamental cellular processes such as cell differentiation, cell proliferation and apoptosis through modulation of gene expression. Critical to understanding the role of miRNAs in this regulation is a method to rapidly and accurately quantitate miRNA gene expression. Existing methods lack sensitivity, specificity and typically require upfront enrichment, ligation and/or amplification steps. The *Direct* miRNA assay hybridizes two spectrally distinguishable fluorescent locked nucleic acid (LNA)-DNA oligonucleotide probes to the miRNA of interest, and then tagged molecules are directly counted on a single-molecule detection instrument. In this study, we show the assay is sensitive to femtomolar concentrations of miRNA (500 fM), has a three-log linear dynamic range and is capable of distinguishing among miRNA family members. Using this technology, we quantified expression of 45 human miRNAs within 16 different tissues, yielding a quantitative differential expression profile that correlates and expands upon published results.

Short noncoding RNA molecules called microRNAs act as potent regulators of gene expression. First discovered in *Caenorhabditis elegans*, the *lin-4* and *let-7* miRNAs were found to regulate the timing of larval developmental stages[1,2]. miRNAs have also been implicated as mammalian developmental regulators in mouse studies characterizing miRNAs in stem cell differentiation[3,4]. Work in *Drosophila melanogaster* identified a cell proliferation–promoting miRNA named *bantam*[5]. Further substantiating a role for miRNAs in cell fate commitment and cell proliferation, several human miRNAs have altered expression in cancer cells[6–9].

miRNAs are transcribed as long primary transcripts within the nucleus where they are cleaved by nuclear ribonuclease III enzyme Drosha into a 60- to 120-nucleotide-long hairpin precursor[10]. The hairpin is exported by a Ran-GTP–dependent exportin 5–mediated pathway[11] into the cytoplasm where it is processed by Dicer into the mature 21–23-nucleotide transcript containing a 5′ phosphate and a 3′ hydroxyl. The mature miRNA is loaded into a multisubunit protein complex, RNA-induced silencing complex (RISC). miRNA-loaded RISC then binds through complete or partial complementarity to the 3′ untranslated regions of target messenger RNAs. miRNA-induced modulation of gene expression can occur through several mechanisms including targeted methylation of genomic DNA, a post-transcriptional translation block or mRNA cleavage and subsequent degradation.

Although the research community has recently seen an explosion of research and new ideas regarding small RNA silencing, the field is relatively nascent in terms of characterizing the universe of miRNAs and their expression profiles in various biological states. According to the miRNA registry (release 6.0; http://www.sanger.ac.uk/Software/Rfam/mirna/index.shtml), of the 227 predicted human miRNAs, the expression of only 131 has been experimentally verified by northern blot, cloning or microarray. Additionally, the total number of miRNAs within a genome is unknown. The short 21-nucleotide nature of these molecules makes them difficult to study via conventional techniques. They are not easily amplified, which makes miRNA microarrays and quantitative PCR technically challenging. Despite these challenges, several groups have undertaken miRNA microarray studies. Most of their approaches are similar in requiring upfront enrichment for small RNAs, reverse transcription, PCR amplification, labeling and clean-up steps. There are a few notable exceptions including the RNA-primed, array-based Klenow enzyme assay (RAKE)[12] and Ambion's *mir*Vana miRNA labeling kit that require only enrichment for small RNAs but do not require amplification. Although the parallelism of arrays is well-suited for large-scale screening, they lack the ability to finely discriminate expression levels and are at best semiquantitative. The 'gold standard' for characterizing miRNA expression is northern blotting, which requires large amounts of RNA and is a relatively insensitive means of measuring expression levels. Thus, sensitive, specific, quantitative and rapid methods for measuring the expression levels of miRNAs would considerably advance the field.

Over the past two decades, advances in single-molecule detection, laser-induced fluorescence (LIF) and fluorescence correlation spectroscopy have provided highly sensitive approaches to study individual macromolecules under physiological conditions[13–15].

[1]US Genomics, 12 Gill Street, Suite 4700, Woburn, Massachusetts 01801, USA. [2]Epic Therapeutics, Inc., 220 Norwood Park, South Norwood, Massachusetts 02062, USA. [3]Novartis Institutes for Biomedical Research, 250 Massachusetts Avenue, 6C-341, Cambridge, Massachusetts 02139, USA. [4]Rx-Gen Inc., 100 Deepwood Drive, Hamden, Connecticut 06517, USA. Correspondence should be addressed to L.A.N. (lneely@usgenomics.com).

RECEIVED 5 AUGUST; ACCEPTED 2 NOVEMBER; PUBLISHED ONLINE 20 DECEMBER 2005; DOI:10.1038/NMETH825

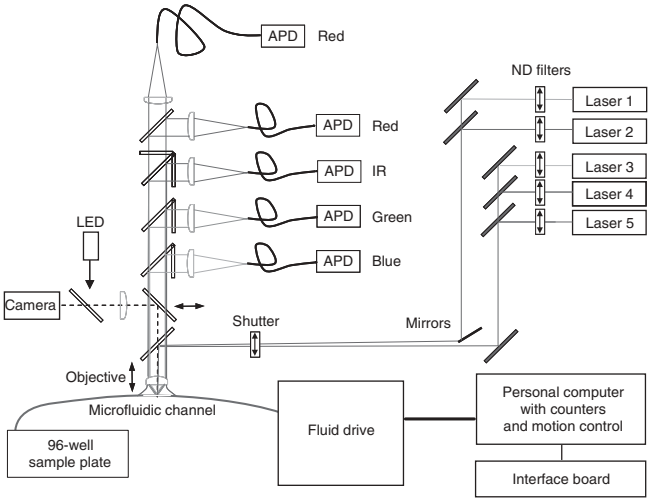

Figure 1 | A schematic diagram of our five laser single molecule detection platform. APD, single-photon avalanche photodiode; ND, neutral density filter.

These single-fluorophore, single-molecule techniques have been routinely used to quantitatively measure properties of molecules in dynamic systems such as protein folding, DNA transcription, DNA binding proteins and molecules in flowing-fluid systems[16–20]. In dual-color fluorescence correlation spectroscopy experiments, individual molecules diffuse into an interrogation volume and a time-dependent cross-correlation provides single-molecule analysis with sensitivities of 10–100 nM[14]. Overall, these studies demonstrate the ability of single-molecule techniques to detect and quantitate the physico-chemical properties of individual biomolecules; however, single-molecule techniques have not previously been used to quantitate miRNA in complex biological samples.

We have developed a single-molecule method for detecting and quantitating miRNAs in biological samples with great sensitivity and specificity. In the present study we demonstrate the sensitivity, specificity and dynamic range of our miRNA assay. We further apply this method to generate a quantitative expression profile of 45 human miRNAs within 16 different human tissues.

RESULTS

Assay design

We built a microfluidic, multicolor confocal laser system capable of counting individual molecules as they flow at high velocity through the system. A schematic of our single-molecule detection platform is shown (**Fig. 1**). Further, we developed a solution-based hybridization assay with femtomolar sensitivity for quantitation of miRNAs using two spectrally distinguishable fluorescently labeled LNA-DNA chimeric probes (**Fig. 2** and **Supplementary Table 1** online).

We quantitated miRNAs by counting the dual-color coincident signals (bursts of photon emission) from the miRNA-hybridized probes (**Fig. 2c**).

miRNA assay sensitivity and dynamic range

To determine the sensitivity and range over which the assay is linear, we conducted hybridization reactions with 0 to 300 pM of a representative miRNA target (*mir-9*) spiked into a complex RNA background (*Escherichia coli* total RNA) and counted the number of coincident events detected. We diluted these reactions fivefold before single-molecule detection. The scattergram shows the number of molecules detected at miRNA run concentrations ranging from 100 fM to 60 pM (**Fig. 3**). The lower limit of quantitation for these assays is 500 fM, which upon fivefold dilution corresponds to a run concentration of 100 fM. The assay is linear over a three-log dynamic range with a coefficient of determination of 0.997.

miRNA assay specificity

Most of the 237 human miRNAs differ by four or more nucleotide bases[21]. There are, however, miRNA families whose members differ by only one or two nucleotide bases. To determine whether our miRNA assay is capable of discrimination among family members, we hybridized *let-7a* probes to *let-7a*, *let-7b*, *let-7c* and *let-7d* miRNA targets in reactions containing 10, 50 or 100 pM of these *let-7* family members. We diluted these reactions tenfold before single molecule detection. We observed an average 40-fold reduction in coincident events between *let-7a* and *let-7b* as well as between *let-7a* and *let-7d* at all of our test concentrations and a threefold reduction in coincident events between *let-7a* and *let-7c* (**Fig. 4**). These results suggest that these probes can be used to discriminate among the four *let-7* family members.

To ensure the coincident events counted were not elevated because of nonspecific or specific binding to higher-molecular-weight RNAs, we hybridized our miRNA probes with 200 ng of poly(A)-enriched mRNAs from 12 of the 16 tissues used within our study (data not shown). In all cases the average coincident event counts were low (less than 50) and the standard deviations for the

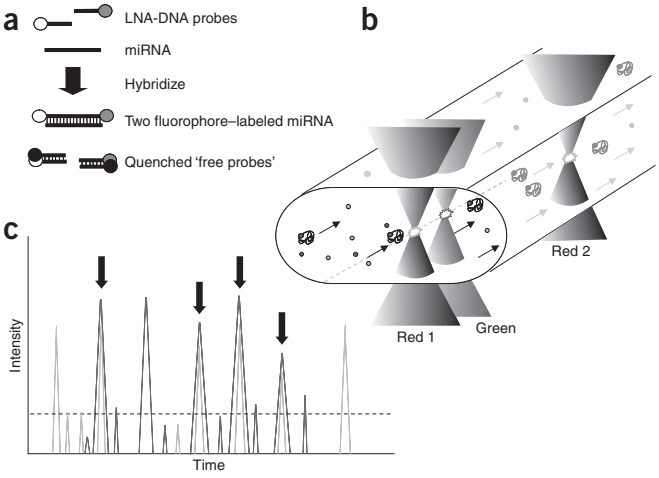

Figure 2 | The single-molecule two-color coincident detection strategy. (**a**) miRNAs were hybridized in solution to two spectrally distinguishable fluorescent LNA-DNA probes. Complementary DNA probes bearing fluorescence quencher molecules were hybridized to the remaining unbound fluorescent probes to minimize coincident events that could be created by free probes simultaneously entering the laser interrogation spots. (**b**) The two fluorophore–labeled miRNAs are flowed by vacuum pressure through a capillary containing a series of femtoliter laser focal volumes. For this study the 532-nm laser spot was focused 2 μm downstream from the first 633-nm spot (Red 1), and the second 633-nm spot (Red 2) was focused 12 μm downstream from the first red spot. The data analysis software uses a standard cross correlation algorithm to measure the flow velocity between the laser spots. (**c**) Fluorescence emission was recorded as spikes in signal intensity over time. Arrows highlight the coincident peaks in photon emission.

four replicate samples were high suggesting random error and therefore suggesting that the probes are not hybridizing to the higher–molecular-weight RNAs.

A human miRNA quantitative expression profile

To demonstrate the utility of the assay for quantitating endogenous miRNAs, we measured the miRNA expression levels of 45 different human miRNAs in 16 different tissues. We incubated 500 ng to 2 μg of human total RNA in the hybridization reactions with 1 nM of each miRNA probe set. For each miRNA target, we prepared three independent standard curves by spiking synthetic miRNA targets into 500 ng of *E. coli* total RNA. All standard curves exhibited strong correlation between the number of detected coincident peaks and the miRNA concentration with the coefficients of determination for 43 of the 45 miRNAs at greater than 0.99 and two at 0.98 (data not shown).

The heat map (**Fig. 5**) shows the quantitative expression pattern measured for each tested human miRNA. The coefficient of variation between the three independent experiments when miRNA expression was observed was less than 20% for 219 of the 245 experiments and less than 25% for all experiments. We observe a broad range of expression levels for the various miRNAs from as little as 45 fg/μg RNA for *mir-187* in prostate to as high as 92,000 fg/μg RNA for *mir-145* in prostate. We were unable to detect expression of the following miRNAs within the 16 tissue total RNAs: *mir-18*, *mir-96*, *mir-129*, *mir-182*, *mir-185*, *mir-218* and *mir-299*. We found *mir-16*, *mir-22*, *mir-145* and *let-7a* to be ubiquitously expressed in our test tissues.

To further characterize the sensitivity of the assay, we tested our ability to quantitate miRNA expression in 50 and 100 ng of tissue total RNA. We selected *mir-22*, *mir-126*, *mir-145* and *mir-191* for this test to represent a range of expression levels, and we quantitated their expression in tissues in which previous work[22] and our own study have indicated their presence at low, moderate and high levels. Hybridization reactions were conducted with 50, 100 and 500 ng of tissue RNA, and for ease of data comparisons, we report the mean number of femtograms of miRNA per microgram total RNA ($n = 3$; **Table 1**). In general, we observed good agreement between the amount of each target miRNA measured with 50, 100 and 500 ng of total RNA with correlation of variation (CV; standard deviation /mean) less than 20% for six of eight experiments and less than 25% for all eight experiments. These data suggest that for most miRNAs 50 ng of tissue total RNA is sufficient for accurate and precise quantitation; however, it should be noted that the higher CV associated with the detection of *mir-126* in pancreas (25% across the 50, 100 and 500 ng samples probed) is likely due to inaccuracy in quantitation within the 50-ng sample.

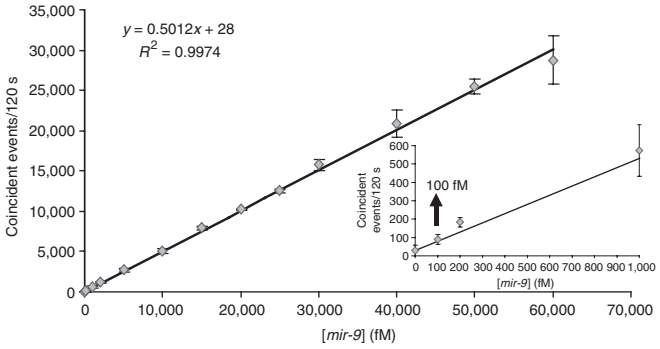

Figure 3 | The *Direct* miRNA assay is sensitive to 500 fM miRNA. A synthetic *mir-9* RNA oligonucleotide, serially diluted from 300 pM to 500 fM, was hybridized in the presence of a complex RNA background (500 ng *E. coli* total RNA) to its complementary Oyster 556 and Oyster 656 LNA-DNA probes. After a 1-h quenching reaction, the fivefold-diluted hybridization reactions were analyzed on our single-molecule detection platform. Inset, an enlarged view of the lower end of the standard curve. The data were fit using an ordinary least squares fit of a simple linear regression model. Error bars, s.d. ($n = 3$).

To corroborate our assay results, we conducted northern blot analyses probing for the expression of four different human miRNAs (*mir-107*, *mir-143*, *mir-145* and *mir-191*) in nine different human tissues. (**Supplementary Fig. 1** online) Linear regression using ordinary least squares analysis indicated that our assay results and northern blot data were strongly correlated with a correlation coefficient of 0.947.

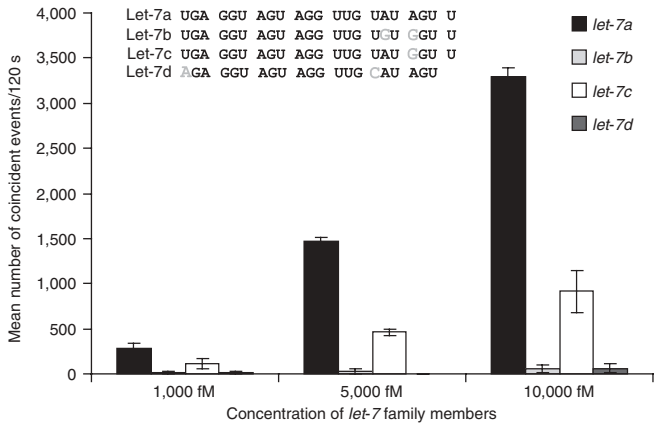

Figure 4 | The *Direct* miRNA assay can be used to specifically detect the target miRNA. LNA-DNA probes designed to have high affinity for *let-7a* were hybridized to four members of the *let-7* family (sequences of the individual family members are indicated). After hybridization and quenching reactions, all samples were diluted tenfold for single-molecule analysis; run concentrations of the samples are indicated. Error bars, s.d. ($n = 3$).

DISCUSSION

Here we present a new single-molecule technique for the quantitation of miRNAs and used this method to quantitate the expression of 45 different miRNAs in 16 human tissues. Above all, we observed measurable miRNA expression across many of our tested tissues, varying broadly across these tissues and consistent with previous studies that have characterized tissue-specific miRNA expression[22,23]. For example, *mir-145* expression varies 90-fold from cervix (90 pg/μg of total RNA) to liver (1 pg/μg of total RNA). Corroborating published literature on miRNA expression, we did observe a few miRNAs whose expression appears confined to a single tissue (*mir-9* and *mir-124a* in brain, *mir-216* in thymus and *mir-122a* in liver) and several miRNAs with no expression in any of our test tissues (*mir-18*, *mir-96*, *mir-129*, *mir-182*, *mir-185*, *mir-218* and *mir-299*)[22]. In addition to measuring amounts of relatively abundant miRNAs, which support published results, we were able to discover and quantitate low levels of miRNA gene expression in tissues that were not previously reported, suggesting that this method is more sensitive than more conventional methods for profiling miRNA expression. For example, we detected *mir-22*

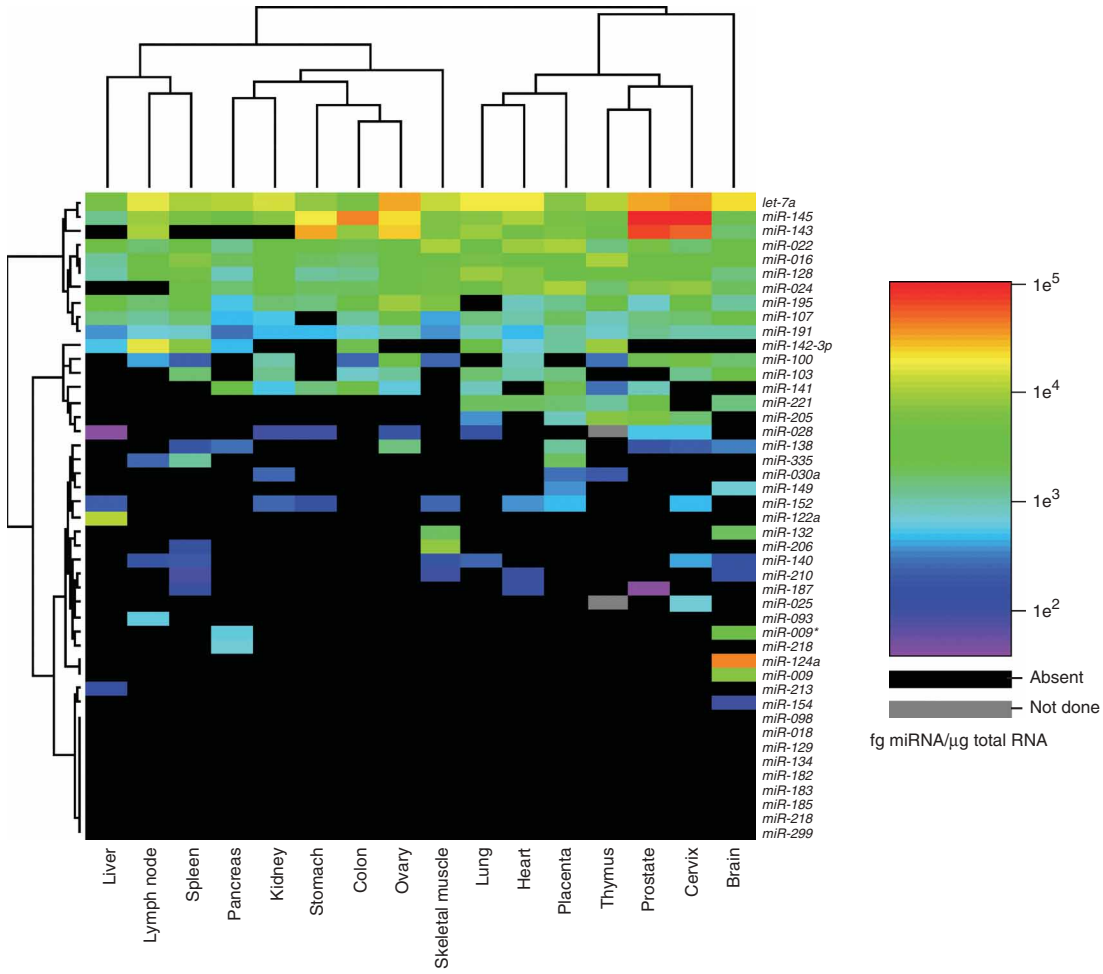

Figure 5 | A human miRNA expression profile that both characterizes and quantifies the tissue-specific expression of 45 different miRNAs within 16 different tissues. The coefficient of variation of the raw coincident event data was less than 25%. 'Absent' indicates there was no reproducibly detectable signal above background.

expression in all of our test tissues; however, via microarray *mir-22* was not detected in cervix, colon, lymph, ovary, pancreas or prostate. We also detected *mir-24* in pancreas, *mir-28* in cervix, *mir-132* in skeletal muscle, and *mir-136* in cervix, prostate and spleen, whereas the expression of all these miRNAs had not been detected by microarray[22]. The apparently enhanced sensitivity with our direct assay is not attributable to quantitation of mature miRNAs, hairpin precursors and/or primary transcripts as we did not observe appreciable probe hybridization to these molecules in northern blot assays and by probing with poly(A)-enriched RNA (data not shown). That the measured levels are a meaningful result is evidenced by the reproducibility of our results, but we cannot at this time confirm the low abundance expression with other techniques such as microarrays and northern blots because of their sensitivity limits.

We compared the levels measured using our miRNA assay to those obtained by northern blotting for a selection of miRNAs. We conducted northern analyses on *mir-107*, *mir-143*, *mir-145* and *mir-191*. We observed strong correlation between our northern blot data and our single-molecule data ($R = 0.947$; **Supplementary Fig. 1**). This suggests that our method provides qualitatively similar information to that obtainable by northern blotting.

Although the utility of single-molecule coincident event detection for the quantitation of mRNAs or identification of unamplified genomic DNA has been demonstrated in previous reports[24,25], this is the first study to apply single-molecule detection to miRNA quantitation. Our method is extremely simple and yields

Table 1 | The *Direct* miRNA assay can accurately quantitate miRNAs in as little as 50 ng of tissue total RNA

		Average fg/µg ± s.d.			
miRNA	Tissue	50 ng	100 ng	500 ng	CV
mir-22	Brain	1,649 ± 102	2,095 ± 622	2,578 ± 193	22%
	Prostate	6,129 ± 526	6,518 ± 510	5,698 ± 84	6%
mir-126	Pancreas	602 ± 3	1,006 ± 11	891 ± 218	25%
	Lung	7,927 ± 655	8,666 ± 1,765	6,906 ± 182	11%
mir-145	Brain	2,170 ± 415	2,054 ± 134	2,114 ± 185	2%
	Heart	10,957 ± 491	11,827 ± 440	10,750 ± 261	5%
	Colon	17,899 ± 308	18,045 ± 540	13,742 ± 545	15%
mir-191	Spleen	816 ± 36	Not determined	845 ± 127	3%

mir-22, *mir-126*, *mir-145* and *mir-191* levels were quantitated in 50, 100 and 500 ng of tissue total RNA. All data was normalized to femtograms of target miRNA per microgram of tissue total RNA and presented as the mean of three independent experiments ± s.d.

reproducible data in a few hours. No preparative enrichment, ligation or target/signal amplification steps are required, and there is no sample clean-up step. This lack of sample manipulation limits the points at which variability could be introduced into the assay and the data. The assay is 96-well and 384-well plate–compatible allowing us to quantitate the expression of hundreds of miRNAs per day. The present form of the assay has not been optimized for specificity, but our data suggest it is capable of discrimination of single nucleotide changes. In particular we observed good discrimination between *let-7a*, *let-7b*, *let-7c* and *let-7d* using *let-7a*–specific probes. Even under particularly permissive binding conditions, a single base change in the target miRNA, which results in a probe hybridizing with a G-T mismatch as seen with the *let-7a* probes hybridizing to *let-7c*, we observed a threefold difference in coincident events.

Though our data suggest that under current assay conditions hybridization of the probes to the hairpin precursor is extremely inefficient (data not shown), we cannot exclude the possibility that we are detecting the presence of hairpin precursor as well.

We have measured the hybridization of our probe sets to poly(A)–enriched mRNAs isolated from 12 of the tissues used in this study. In all cases we did not detect a substantial number of coincident events in the samples, which suggests that either we were not efficiently hybridizing them to the primary miRNA transcript or the transcript is not abundant. The lack of coincident events detected also indicates the probes are not hybridizing coincidentally to a nonspecific mRNA target.

The quantitative nature of the data is unique, yielding an accurate and precise amount of miRNA present in tissue total RNA, which is highly reproducible for any given miRNA in a particular tissue; we were able to precisely and repeatedly measure the amount of an miRNA over multiple experiments spanning several months. The accuracy of the method is evidenced by strong correlation between measured amounts of miRNA and northern blot data. The ability to measure the precise amount of a particular miRNA opens up the possibility of detecting subtle changes in miRNA expression that may not be observable by other techniques that measure bulk signal, such as northern blots and microarrays. We are now exploring and extending the potential of this method to quantitate miRNA amounts in diseased tissues.

METHODS

Oligonucleotide and LNA probes and synthetic miRNA target validation. US Genomics (USG) designed chimeric LNA-DNA probes complementary to publicly available miRNA target sequences using in-house design tools. The fluorescently modified chimeric LNA-DNA probes (Proligo or Exiqon), DNA quencher probes containing A-quenchers (Exiqon) and synthetic miRNA templates (Integrated DNA Technologies) were synthesized and purified. We determined the concentrations and stoichiometry of dye-label to oligo by measuring the oligonucleotide's absorbance from 650 nm to 230 nm on a Cary UV-visible spectrophotometer (Varian).

miRNA assay. We pooled First Choice Human total RNA (Ambion) from two to three sources for each tissue studied. Hybridization reactions for the calibration curves consisted of 1 nM probes, 1–100 pM of serially diluted synthetic miRNA target, 500 ng of *E. coli* total RNA and 0.5 μl of RNAse Inhibitor (USB Corporation) in 1× USG hybridization buffer. Human total RNA hybridization reactions consisted of 500 ng to 2 μg of human tissue total RNA, 1 nM of LNA probes and 0.5 μl of RNAse inhibitor in 1× USG hybridization buffer. We prepared specificity controls using 200 ng of poly(A)-enriched mRNA isolated from brain, cervix, colon, heart, kidney, liver, lung, lymph node, placenta, prostate, skeletal muscle and stomach (Ambion). We sealed the 96-well plates with Microseal lids (BioRad) and incubated them at 80 °C for 5 min followed by a 2-h incubation at 55 °C. We chilled the plate and added DNA quencher probes to a final concentration of 1.3 nM. We incubated the quenching reactions at 40 °C for 1 h. The samples were then diluted in USG dilution buffer A tenfold before single-molecule analyses.

Single molecule–detection platform. We used a Trilogy confocal laser-induced fluorescence detector from USG to perform single-molecule counting experiments. The instrument allows four-color fluorescent detection in a microfluidic flow stream as previously described[26], with engineering modifications to automate sample handling and delivery (**Fig. 1**). Optically this system is similar to those described by others[27,28]. At the beam waist, the focused spots have a diameter of approximately 1 μm, and they are arrayed along the capillary (**Fig. 2b**). These highly focused spots permit fluorescent excitation of a very small sample volume (~1 fl) within the capillary. This limits the noise produced by Raman and Rayleigh light scattering and background fluorescence from the biological samples.

Data analysis—coincident event counting. To detect and quantitate molecules of interest we used a coincident event detection strategy[15]. Target molecules containing two fluorescent probes, one labeled with Oyster 556, referred to as the 'green probe', and the other labeled with Oyster 656, referred to as the 'red probe', pass through the femtoliter laser excitation/detection volumes (Red1, Green and Red2) and emit photons (**Fig. 2a**). We recorded the photon bursts emanating from the laser interrogation volume in 1-ms time intervals. The laser spots are arrayed within the microfluidic channel as shown in (**Fig. 2b**). Using a method previously described by others[29], we used cross-correlation between the two red channels to measure the flow velocity of the fluorescently labeled molecules. We focused the 633 nm laser 2 μm upstream of the 532 nm laser. The offset of the laser focal volumes eliminates spectral crosstalk. Our data analysis software accounts for the offset and synchronizes the data allowing a dual fluorescently labeled molecule to be counted as a coincident event. The data analysis method counts the number of coincident events above an established threshold (**Fig. 2c**). More specifically, we counted the number of time periods during which the signal from each of two fluorescence channels exceeded some fixed value for that channel.

Data analysis—miRNA quantitation. We prepared three independent standard curves containing 1, 2, 5, 10, 25, 50, 75 and 100 pM of synthetic miRNA spiked into a complex RNA background (*E. coli* total RNA). In addition we prepared six no-target controls (probes and *E. coli* total RNA background) for each miRNA. We diluted all samples tenfold before single-molecule interrogation. We calculated 95% confidence intervals based on a one-tailed Student's t-test assuming unequal variances, for the

negative controls and for each data point in the calibration curve. The lower limit of quantitation was defined as the first data point on the calibration curve that lies above the upper confidence limit of the 95% confidence interval for the no-target controls and has a CV ($n = 3$) of 20% or less. Linear regression analyses using ordinary least squares estimations were conducted in Origin 6.0 (OriginLab Corporation).

If the coincident event numbers counted in the tissue total RNA from three independent experiments had a coefficient of variation less than 20% and a lower confidence limit of the 95% confidence interval above the upper limit for the 95% confidence interval of the zero target control, we deemed the miRNA (or a closely related family member) as expressed and calculated the concentration of the miRNA within that tissue. In instances in which 500 ng of total RNA yielded a mean coincident event number with a CV of 20% or less but not above the upper 95% confidence limit of our zero target control, we repeated the experiments using 1–2 μg of total RNA. All results were normalized to femtograms of miRNA measured per microgram of total tissue RNA ± s.d.

Hierarchical clustering of miRNA expression data. Expression data was floored at the detection threshold (15 fg) and log-transformed.

Hierarchical clustering using Ward's algorithm and the Euclidean distance metric was performed and a heat map was created in the R statistical environment[30].

Additional methods. Experimental details on the single molecule–detection platform, coincident event counting strategy and northern blotting are available in **Supplementary Methods** online. The sequences of the LNA-DNA chimeric probes used in this study are available in **Supplementary Table 1**.

Note: Supplementary information is available on the Nature Methods website.

ACKNOWLEDGMENTS

We thank our collaborator A.C. Eklund for generating the heat maps and conducting the hierarchical clustering and M. Barth for help preparing the figures. We thank all of our colleagues at US Genomics especially D. Hoey, R. Gilmanshin, J. Larson, E. Nalefski and A. Maletta for fostering fruitful scientific discussion. We thank L. Kunkel, F. Boeckman and D. Whitney for critical review of the manuscript.

COMPETING INTERESTS STATEMENT

The authors declare competing financial interests (see the *Nature Methods* website for details).

Published online at http://www.nature.com/naturemethods/
Reprints and permissions information is available online at http://npg.nature.com/reprintsandpermissions/

1. Lee, R.C., Feinbaum, R.L. & Ambros, V. The *C. elegans* heterochronic gene lin-4 encodes small RNAs with antisense complementarity to *lin-14*. *Cell* **75**, 843–854 (1993).
2. Reinhart, B. *et al.* The 21-nucleotide *let-7* RNA regulates developmental timing in *Caenorhabditis elegans*. *Nature* **403**, 901–906 (2000).
3. Houbaviy, H.B., Murray, M.F. & Sharp, P.A. Embryonic stem cell-specific MicroRNAs. *Dev. Cell* **5**, 351–358 (2003).
4. Chen, C.Z., Li, L., Lodish, H.F. & Bartel, D.P. MicroRNAs modulate hematopoietic lineage differentiation. *Science* **303**, 83–86 (2004).
5. Brennecke, J., Hipfner, D.R., Stark, A., Russell, R.B. & Cohen, S.M. *bantam* encodes a developmentally regulated microRNA that controls cell proliferation and regulates the proapoptotic gene hid in *Drosophila*. *Cell* **113**, 25–36 (2003).
6. Michael, M.Z., O' Connor, S.M., van Holst Pellekaan, N.G., Young, G.P. & James, R.J. Reduced accumulation of specific microRNAs in colorectal neoplasia. *Mol. Cancer Res.* **1**, 882–891 (2003).
7. Calin, G.A. *et al. MicroRNA profiling reveals distinct signatures in B cell chronic lymphocytic leukemias*. *Proc. Natl. Acad. Sci. USA* **101**, 11755–11760 (2004).
8. He, L. *et al.* A microRNA polycistron as a potential human oncogene. *Nature* **435**, 828–833 (2005).
9. Johnson, S.M. *et al. RAS is regulated by the let-7 microRNA family*. *Cell* **120**, 635–647 (2005).
10. Kim, V.N. MicroRNA biogenesis: coordinated cropping and dicing. *Nat. Rev. Mol. Cell Biol.* **6**, 376–385 (2005).
11. Yi, R., Qin, Y., Macara, I. & Cullen, B.R. Exportin-5 mediates the nuclear export of pre-microRNAs and short hairpin RNAs. *Genes Dev.* **17**, 3011–3016 (2003).
12. Nelson, P.T. *et al.* Microarray-based, high-throughput gene expression profiling of microRNAs. *Nat. Methods* **1**, 155–161 (2004).
13. Yanagida, T., Kitamura, K., Tanaka, H., Hikikoshi Iwane, A. & Esaki, S. Single molecule analysis of the actomyosin motor. *Curr. Opin. Cell Biol.* **12**, 20–25 (2000).
14. Schwille, P., Bieschke, J. & Oehlenschlager, F. Kinetic investigations by fluorescence correlation spectroscopy: the analytical and diagnostic potential of diffusion studies. *Biophys. Chem.* **66**, 211–228 (1997).
15. Li, H., Ying, L., Green, J.J., Balasubramanian, S. & Klenerman, D. Ultrasensitive coincidence fluorescence detection of single DNA molecules. *Anal. Chem.* **75**, 1664–1670 (2003).
16. Schwille, P., Kummer, S., Heikal, A.A., Moerner, W.E. & Webb, W.W. Fluorescence correlation spectroscopy reveals fast optical excitation-driven intramolecular dynamics of yellow fluorescent proteins. *Proc. Natl. Acad. Sci. USA* **97**, 151–156 (2000).
17. Anazawa, T., Matsunaga, H. & Young, E.S. Electrophoretic quantitation of nucleic acids without amplification by single-molecule imaging. *Anal. Chem.* **74**, 5033–5038 (2002).
18. Ambrose, W.P. *et al.* Detection system for reaction-rate analysis in a low-volume proteinase-inhibition assay. *Anal. Biochem.* **263**, 150–157 (1998).
19. Dovichi, N.J., Martin, J.C., Jett, J.H., Trkula, M. & Keller, R.A. Laser-induced fluorescence of flowing samples as an approach to single-molecule detection in liquids. *Anal. Chem.* **56**, 348–354 (1984).
20. Dundr, M., McNally, J.G., Cohen, J. & Misteli, T. Quantitation of GFP-fusion proteins in single living cells. *J. Struct. Biol.* **140**, 92–99 (2002).
21. Miska, E.A. *et al.* Microarray analysis of microRNA expression in the developing mammalian brain. *Genome Biology* **5**, R71.1–R71.15. (2004).
22. Baskerville, S. & Bartel, D.P. Microarray profiling of microRNAs reveals frequent coexpression with neighboring miRNAs and host genes. *RNA* **11**, 241–247 (2005).
23. Barad, O. *et al.* MicroRNA expression detection by oligonucleotide microarrays: System establishment and expression profiling in human tissues. *Genome Res.* **14**, 2486–2494 (2004).
24. Korn, K. *et al.* Gene expression analysis using single molecule detection. *Nucleic Acids Res.* **31**, e89 (2003).
25. Castro, A. & Williamson, J.G.K. Single molecule detection of specific nucleic acid sequences in unamplified genomic DNA. *Anal. Chem.* **69**, 3915–3920 (1997).
26. Chan, E.Y. *et al.* DNA mapping using microfluidic stretching and single-molecule detection of fluorescent site-specific tags. *Genome Res.* **14**, 1137–1146 (2004).
27. Eigen, M. & Rigler, R. Sorting single molecules: applications to diagnostics and evolutionary biotechnology. *Proc. Natl. Acad. Sci. USA* **91**, 5740–5747 (1994).
28. Nie, S., Chiu, D.T. & Zare, R.N. Real time detection of single molecules in solution by confocal fluorescence microscopy. *Analytical Chemistry* **67**, 2849–2857 (1995).
29. Brinkmeier, M., Dorre, K., Stephan, J. & Eigen, M. Two beam cross correlation: A method to characterize transport phenomena in micrometer-sized structures. *Anal. Chem.* **71**, 609–616 (1999).
30. R Development Core Team. *R: A language and environment for statistical computing*, R foundation for computing. Vienna, Austria (2005) ISBN 3-900051-07-0.